

THE APPLICATION OF AFM FOR BIOLOGICAL SAMPLES IMAGING

D. CHICEA^{*}, B. NEAMTU^a, R. CHICEA^a, L. M. CHICEA^a

Physics Dept., University Lucian Blaga of Sibiu, Dr. Ion Ratiu Str. 7-9, Sibiu, 550012, Romania,

^a“VICTOR PAPILIAN” Medical School, University Lucian Blaga of Sibiu

The Atomic Force Microscopy (AFM) is a technique that is currently used to reveal details on surfaces using different scanning techniques. The biological cells, as opposed to hard condensed matter samples are soft and do not adhere well to surfaces, therefore imaging soft condensed matter samples requires certain precautions. This article presents details and results on using AFM for imaging red blood cells to diagnose spherocytosis and human serum albumin.

(Received July 14, 2010; accepted after revision November 5, 2010)

Keywords: Atomic Force Microscopy, Red Blood Cells, Human Serum Albumin, Spherocytosis

1. Introduction

Living cells, as opposed to hard condensed matter samples are soft and do not always adhere well to surfaces. The typical size of cells is a few microns while the proteins are smaller, in the range of tens of angstroms.

Living cells are divided into two types - prokaryotic and eukaryotic and this division is based on internal complexity. The eukaryotic cells are highly structured and include the cells of protozoa, higher plants and animals. These cells are larger than the cells of bacteria, and have developed specialized packaging and transport mechanisms that are required to support their larger size. The prokaryotic cells are simple in structure, with no recognizable organelles. They have an outer cell wall that gives them shape. Under the rigid cell wall is the cell membrane. The cytoplasm enclosed within the cell membrane does not exhibit complex structure when imaged by electron microscopy.

Studying the living cells and the interaction of the living cells with the environment or different stimuli is tremendously important in developing medication for the countless many diseases that affect human life. Surface characteristics such as hydrophobicity, surface energy, surface texture or patterning at various length scales, surface charge, and chemical composition are all known to play key roles in governing cell adhesion and growth [1]. In the last decades nanoparticles were extensively considered for biomedical applications because the living cells have dimensions of the order of microns and parts of the order of tens to hundreds of nanometers. For this reason it was natural to imagine that nanoparticle structured materials can be used in many ways to investigate, to modify living cells or to deliver certain substances or drugs to them without perturbing much the cells. Thus many practical applications were developed in the last years and are nicely presented in [2, 3] and in many other review papers, not cited here.

The macroscopic response of cells in contact with soft amorphous materials in vitro has long been of considerable interest for medical applications. In spite of that, examination of such responses still remains the basis of early stage assessment within the medical device industry of the viability of implants. Based on experience of these phenomena, criteria for the likely compatibility of materials in contact with animal tissue have been evolved, despite the apparent complexity of in vivo responses, as presented in [4]. In [5], both conventional phenotypic and contemporary transcriptomic analysis techniques were combined to examine the interaction of

^{*} Corresponding author: dan.chicea@ulbsibiu.ro

cells with a homologous series of copolymer films that vary in terms of surface hydrophobicity. Many other examples can be added.

Among complex investigation techniques, cell imaging remains between the most frequently used. In order to keep the cells alive during their interaction with the stimuli, the imaging system must interact as less as possible with the cell. Optical microscopy appears most suited for this purpose and the history of using this technique spreads over centuries. The standard optical microscopy, also called bright field microscopy, has limitations though. The limitations lie in three areas: the technique can only image dark or strongly refracting objects effectively. The second limitation is caused by diffraction as it limits resolution to approximately 0.2 microns. The third limitation is caused by the out of focus light from points outside the focal plane that blurs the image.

Live cells do not have sufficient contrast to be studied successfully. The internal structures of the cell are colorless and mostly transparent. The most common way to increase contrast is to stain the different structures with selective dyes, but this involves killing and fixing the sample. Staining may also introduce artifacts, apparent structural details that are caused by the processing of the sample and are thus not a characteristic feature of the specimen.

These limitations have all been overcome to a certain extent by specific microscopy techniques that can non-invasively increase the contrast of the image. In general, these techniques make use of differences in the refractive index of cell structures. This creates a difference in phase of the light passing through. The human eye is not sensitive to this difference in phase but several optical solutions have been created to change this difference in phase into a difference in amplitude (light intensity) [7-8]. The difference in densities and composition within the imaged objects give rise to changes in the phase of light passing through them, hence they are sometimes called "phase objects". The phase-contrast technique makes these structures visible and allows their study while the specimen keeps being alive. Other improvements of the microscopy technique are: differential interference contrast microscopy, interference reflection microscopy, fluorescence microscopy, confocal microscopy, near-field scanning, stimulated emission depletion, photo-activated localization microscopy [9], structured illumination.

An alternative technique that can be used to assess the submicron particle size is the Atomic Force Microscopy (AFM). The AFM technique can be used to image and measure objects that are considerable smaller than the visible light wavelength. One of the papers that reports using AFM even for nanoparticle sizing is [10]. A comparison of the TEM with the AFM results is presented in [11]. The results in [10] reveal that the AFM measured nanoparticle diameter appears to be reduced with 20% and the standard deviation appears to be increased with 15%. The differences in the diameter and in the standard deviation findings were associated with the AFM tip and the nanoparticle concentration on the substrate.

The AFM technique and the results using it in imaging cells and proteins are presented in the following section.

2. Experimental

The atomic force microscope (AFM) is a scanning probe microscope. The AFM uses a flexible cantilever as a type of spring to measure the force between the tip and the sample. The basic idea of an AFM is that the local attractive or repulsive force between the tip and the sample is converted into a deflection of the cantilever. The cantilever is attached to a rigid substrate that can be held fixed, and depending whether the interaction at the tip is attractive or repulsive, the cantilever will deflect towards or away from the surface [12].

The cantilever deflection is converted into an electrical signal to produce the images. The detection system uses a laser beam that is reflected from the back of the cantilever onto a detector. The optical lever principle is used. This states that a small change in the bending angle of the cantilever is converted to a precisely measurable deflection in the position of the reflected spot. By scanning the sample line by line and using a calibration file for each scanner a topography image of the surface is reconstructed by the software that drives the scanning process.

The AFM that was used in the work reported here is an Agilent 5500 type. The scanning mode was ACAFM. A soft tip, having the spring constant equal to 5 N/m was used at low force amplitude. As the cells or proteins undergo a Brownian motion in suspension, scanning in liquid can not be used for cell imaging, also the Agilent 5500 microscope can scan in liquid.

Sample preparation is crucial in order to get useful AFM images. The samples must be thin enough to have a single layer of the objects that are studied, whether they are micron sized cells or nanometer sized particles.

The second condition that a sample for AFM imaging must fulfill is that the objects to be imaged must adhere well to the surface and remain in the same position during the scanning process, otherwise they will be moved by the tip of the cantilever, thus producing artifacts.

The first type of cells that were imaged using AFM was the Red Blood Cells (RBC). RBCs, also referred to as erythrocytes, are the most common type of blood cell and the vertebrate organism's principal means of delivering oxygen to the body tissues via the blood flow. They take up oxygen in the lungs or gills and release it while squeezing through the body's capillaries. The RBCs cytoplasm is rich in hemoglobin, thus having a red color. In the hemoglobin composition there is an iron-containing biomolecule that can bind oxygen. In humans, mature RBCs are flexible biconcave disks (doughnut shape) that lack a cell nucleus and most organelles. The cells are produced in the bone marrow and circulate for about 100–120 days in the body before their content is recycled by macrophages [13].

Anemia is a decrease in normal number of RBCs or less than the normal quantity of hemoglobin in the blood. Spherocytosis is an auto-hemolytic anemia characterized by the production of RBCs that are sphere-shaped, rather than bi-concave disk shaped. The sphere-shaped red blood cells are known as spherocytes. These cells are more prone to physical degradation. The misshapen but otherwise healthy red blood cells are mistakenly considered by the spleen to be old or damaged red blood cells and it thus constantly destroys them, causing a cycle whereby the body destroys its own blood supply [14].

A drop of blood sampled from a patient with spherocytes was deposited on a glass microscope slide and stretched with another microscope slide edge to form a very thin layer. The thin layer was left for 2 hours at 22°C in 40% humidity air to evaporate. This was the first sample that was imaged using the AFM microscope. The same sample preparation procedure was used for a drop of blood sampled from a healthy donor that checked in for a periodic health control.

The second type of sample that was studied using the AFM microscope was a protein. The protein was human serum albumin (HSA). It is the most abundant protein in human blood plasma and is produced in the liver. Albumin comprises about half of the blood serum protein. It is soluble and monomeric. The reference range for albumin concentrations in blood is 30 to 50 g/L. It has a serum half-life of approximately 20 days and a molecular mass of 67 kDa [15]. The size of the HSA was studied using the dynamic light scattering (DLS). The albumin globule has the most compact configuration (Stokes diameter 59–62 Å) at physiological pH 7.4. The changes in pH, both increase to 8.0 and decrease to 5.4, result in the growth of globule size to 72–81 Å [16-17]. At acidic shift of pH an additional peak arises in the correlation spectra caused by the light scattering on the structures with the Stokes diameters of 29–37 Å. This result is consistent with the sizes of the albumin subdomains [16, 17].

Another size and shape investigation of HSA in 150 mM NaCl aqueous solutions was studied by small-angle neutron scattering [18]. The radius of gyration of albumin molecule was found to be 27.4 ± 0.35 Å. A compact sphere would have a smaller radius of gyration, whereas in the cigar-shaped model for the molecule, about 136 Å long, would have a larger radius of gyration [18]. A prolate ellipsoid less than 110 Å long or an oblate ellipsoid about 85 Å in diameter are the possible forms of albumin molecule consistent with the results obtained [18].

The sample preparation for imaging HSA using AFM was slightly different than for imaging RBCs. A small drop of diluted HSA, 2% volume ratio, was deposited on a freshly cleaved mica substrate. It was stretched on the substrate using a sharp edge and allowed to evaporate for 4 hours at 22°C in 40% humidity air.

The results of the AFM measurements on the two types of samples are presented in the next section.

3. Results and discussion

The sample with blood from a healthy donor, prepared as described in the previous section, was first imaged using an optical microscope (bright light image) having a 40X objective and a 3.15 Megapixel CCD camera attached on it. The normal RBCs appear bright in the middle. They appear in such a manner because they act like a divergent lens in visible light, as their middle displays an optical pass smaller than their contour, when they are attached to a plane surface parallel to the plane and the light direction is perpendicular to the surface. This typical aspect in visible light, caused by their doughnut shape, is presented in Fig. 1.

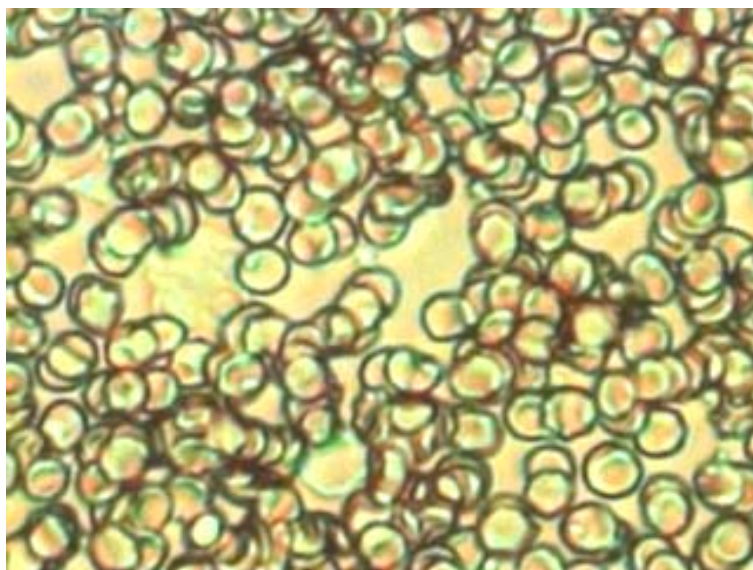


Fig. 1. The typical aspect of healthy RBCs in visible light.

In the blood sample taken from a patient with spherocytosis some but not all of the RBCs have a spherical shape. In an optical microscope image the spherical RBCs do not display the lighter center, but are opaque, as presented in [19].

The optical microscope image is a differential diagnosis criteria and helps the physician to establish whether the anemia is a spherocytosis anemia or has a different cause.

The optical microscopy image strongly differs from one microscope type to another, of the magnification and of the staining as well, as can be noticed examining Fig. 1 and [19].

The sample with blood from the donor having spherocytosis was attached to the AFM plate and for the beginning a large area ($50\ \mu\text{m} \times 50\ \mu\text{m}$) surface scan was carried on. The flat image of the surface topography is presented in Fig. 2.

Examining Fig. 2 we notice that the image, having a considerable larger magnification than the optical image in Fig. 1, reveals both normal (doughnut shaped) and spherical RBCs. The dark spots in the middle of the normal RBCs stand for lower areas, as indicated by the depth scale ruler on the right side of Fig. 2, while the lighter areas in the middle of some RBCs indicate upper areas, thus spherical RBCs.

A higher resolution scan of the RBCs in the middle of the area in Fig. 2, $20\ \mu\text{m} \times 20\ \mu\text{m}$ wide, is presented in Fig. 3.

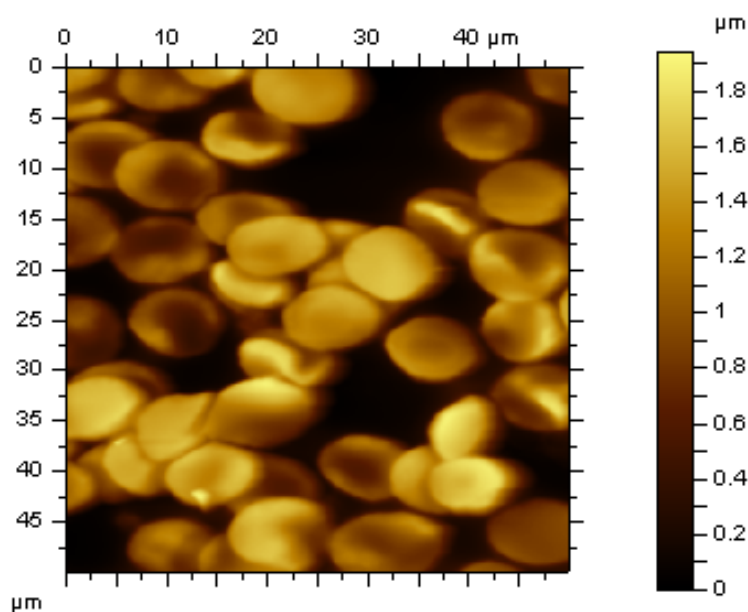


Fig. 2. RBCs on a microscope glass slide substrate, both normal and spherical.

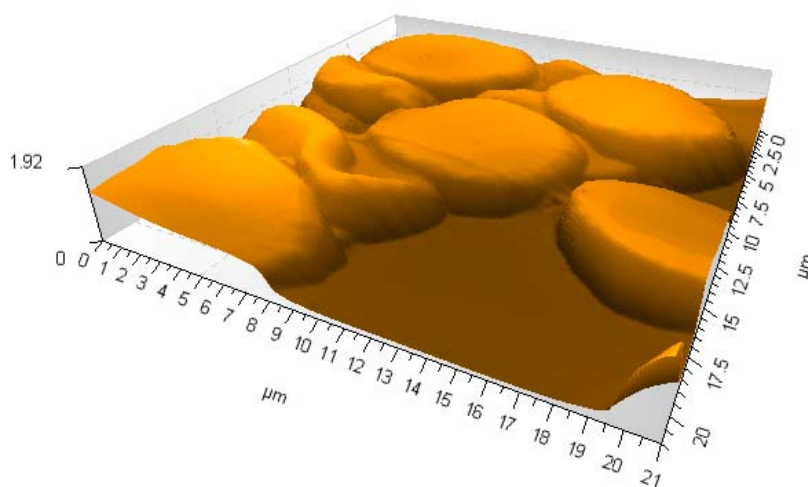


Fig. 3. RBCs on a microscope glass slide substrate; a 20 μm x 20 μm wide area, 3D rendering type.

Examining Figs. 2 and 3 we notice beyond any doubt that some of the RBCs have a different shape than the typical doughnut shape, as displayed by the RBCs on the right of Fig. 3. Moreover, the image has a considerably bigger resolution than the optical image, a typical one being presented in Fig. 1

The second sample, HSA prepared on a mica substrate as described in the second section was attached to the AFM plate and a relatively large area compared with the size of the object being investigated, 2 μm x 2 μm was scanned. The proteins were relatively dense on the substrate; therefore a bigger resolution scan of a smaller area, 0.5 μm x 0.5 μm was conducted. A 3D rendering type image is presented in Fig. 4.

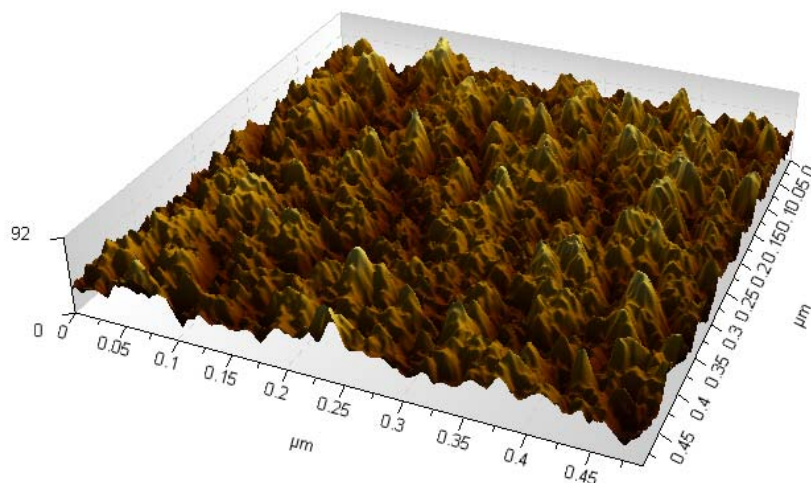


Fig. 4. A 3D rendering type image of a $0.5 \mu\text{m} \times 0.5 \mu\text{m}$ area on the sample. HSA on freshly cleaved mica substrate.

Examining Fig. 4 we notice that even at a 2% (volume ratio) concentration there are many albumin molecules on the small area that was imaged and assessing the protein dimension from a 3D image is not accurate. A better way to assess the particle dimension on a surface is to extract vertical profiles. Several vertical profiles extracted from the topography of the area presented in Fig. 4 are presented in Figs. 5 and 6.

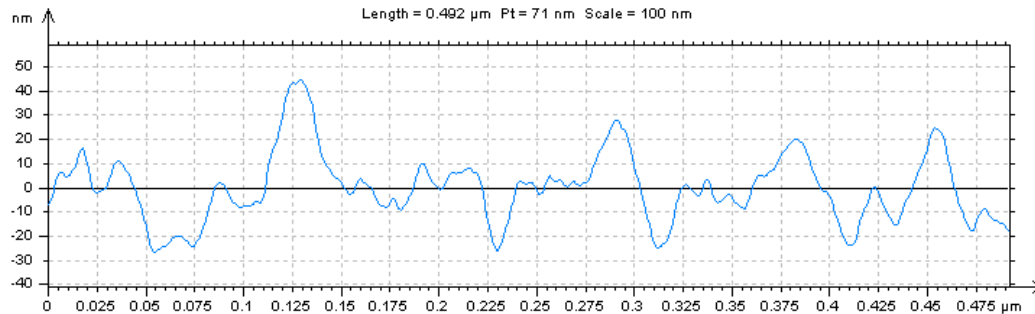


Fig. 5. a vertical profile extracted from the scanned area presented in Fig. 4.

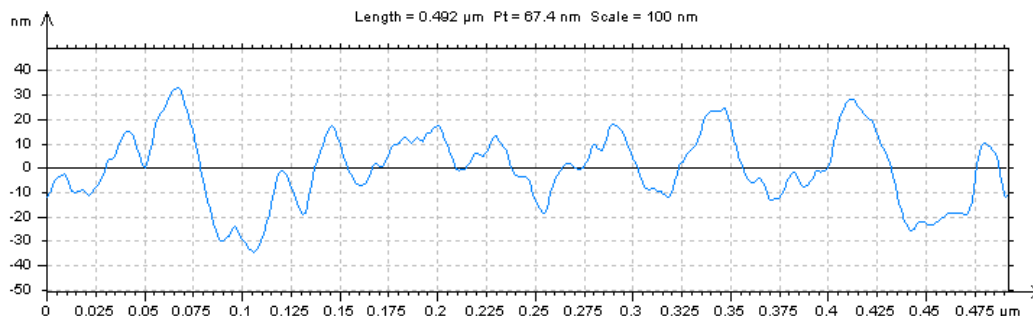


Fig. 6. another vertical profile extracted from the scanned area presented in Fig. 4.

The Z difference between two points in the vertical profile was considered rather than the x or y difference because the cantilever tip is not ideal but has a radius of at least 40 nm and increases during scanning, as the tip wears out. When imaging a small object using a tip with a

comparable dimension, artifacts can be produced, as presented in detail in [20], but using the vertical differences leads to precise dimension measurements.

Examining Figs. 5 and 6 we notice that the difference between the base (lowest) line, which represents the mica substrate and the top of the albumin molecules in the profile is around 50 nm.

When interpreting these results we must have in mind that the HSA complex molecule is not spherical but can be described as an ellipsoid [18] and different values of the size were reported [16 – 18], strongly depending on the pH of the solution. Different orientations of the HSA molecule attached on the substrate can be considered, therefore the larger differences between the base line and the top of the peaks in the vertical profile should be considered as the size along the biggest dimension of the protein. With this in mind, we notice that the dimension we found from the AFM measurements, that is around 50 nm, is consistent with the HSA dimension reported in [16-17], but smaller than neutron scattering result found for the radius of gyration in the cigar or ellipsoid model and bigger than in the spherical model [18].

If we assume that the ellipsoid model [18] is correct and that the HSA globule can have different orientation on the mica surface, we can consider that the smaller Z differences between the lowest line and the smaller peaks represent the dimension of the smaller ellipsoid axis. Figs. 5 and 6 indicate that the dimension of the HAS globule across the small axis is around 25-30 nm.

Moreover, the measurements reported in [16 – 18] were carried on with the HSA in liquid, at physiological or shifted pH and the influence of the pH was clearly stated. The AFM measurements were conducted on dry samples, therefore the differences in the size we found, as compared with the DLS and neutron scattering measurements results can be attributed both to the environment and to the method.

4. Conclusions

Two biological samples were analyzed using AFM, RBCs from a patient having spherocytosis and HSA.

The RBC sample preparation for AFM imaging was identical with the sample preparation for optical imaging, that is a small drop was stretched on a glass microscope slide using the edge of another microscope slide and allowed to dry.

The AFM image was compared with an optical microscope image (in bright light mode). The resolution of the AFM is much bigger than the optical microscope image and a 3D image can be easily obtained after an AFM scan, therefore the spherical or different than the doughnut shape of some of the RBCs was made evident without any doubt. This proves that the AFM technique, also more time consuming than optical microscope imaging, is a precise technique that can be used to clearly identify spherocytosis.

The other biological sample that was imaged and analyzed using AFM is human albumin, also named HSA. The sample preparation is different of the sample preparation for RBCs, because the size of HSA is much smaller than the size of RBCs. For that reason a much flatter surface must be used as a substrate, in order to avoid artefacts. A freshly cleaved mica substrate was used for stretching a very thin layer of albumin molecules and it fulfils that condition. The HSA was imaged using AFM and vertical profiles were extracted from the scan. The differences between the coordinates of the top of the peaks and the base line are the dimension of the HSA molecule. The results we found are in good agreement with the results of the DLS and neutron scattering experiments, confirming that the HAS molecule can be modelled as an ellipsoid with the axes around 30 μm and 50 μm respectively. The HSA molecule was imaged on a dry substrate and this can explain the differences in the size of the axis we found, as compared with the results reported in [16 – 18]. Nevertheless, these results prove that the AFM can successfully be used to image and measure nanometer sized biological objects.

Acknowledgements

We are especially indebted to Dr. Gerald Kada of AGILENT for fruitful discussions and training.

References

- [1] Y. Ito, *Biomaterials* **20**, 2333 (1999).
- [2] O.V. Salata, *Journal of Nanobiotechnology* **2**, 3, (2004), doi:10.1186/1477-3155-2-3.
- [3] Q.A. Pankhurst., J. Connolly, S.K. Jones, J. Dobson, *J. Phys. D*, **36**, R167 (2003).
- [4] B. Rihova, *Adv. Drug Delivery Rev.* **21**, 157 (1996).
- [5] L. T. Allen, E. J. P. Fox, I Blute, Z. D. Kelly, Y. Rochev, A. K. Keenan, K. A. Dawson, W. M. Gallagher, *PNAS* **100**(11), 6331 (2003).
- [6] S. Bradbury, B. Bracegirdle, *Introduction to Light Microscopy*, BIOS Scientific Publishers (1998)
- [7] F. Zernike, *Physica*: **9**, 686 (1942).
- [8] F. Zernike, *Physica*: **9**, 974 (1942).
- [9] E. Betzig, G. H. Patterson, R. Sougrat, O. W. Lindwasser, S. Olenych, J. S. Bonifacino, M. W. Davidson, J. Lippincott-Schwartz, H. F. Hess, *Science* **313**(5793), 1642 (2006), DOI: 10.1126/science.1127344
- [10] F. Zhang, S.W. Chan, J. E. Spanier, E. Apak, Q. Jin, R. D. Robinson, I. P. Herman, *Appl. Phys. Lett.* **80**, 27 (2002); doi:10.1063/1.1430502.
- [11] L. M. Lacava, B. M. Lacava, R. B. Azevedo, Z. G. M. Lacava, N. Buske, A. L. Tronconi and P. C. Morais, *Journal of Magnetism and Magnetic Materials*, **225**(1-2), 79 (2001).
- [12] <http://www.jpk.com/general-scanning-probe-microscopy.431.html>
- [13] F. Pierigè, S. Serafini, L. Rossi, M. Magnani, *Advanced Drug Delivery Reviews* **60**(2), 286 (2008), doi:10.1016/j.addr.2007.08.029.
- [14] Table 12-1 in: R. Sheppard, V. Kumar, A. K. Abbas, F. Nelson, R. Mitchell, *Robbins Basic Pathology*, 8th edition, Saunders, Philadelphia, 2007, ISBN 1-4160-2973-7.
- [15] M.H. Beers, ed. in chief, *Merk Manual of Diagnosis and Therapy*, 18th edition, The Merk Publishing Group, New Jersey, 2006
- [16] A. I. Luik, Yu. N. Naboka, S. E. Mogilevich, T. O. Hushcha and N. I. Mischenko, *Spectrochimica Acta Part A: Molecular and Biomolecular Spectroscopy*, **54**(10), 1503 (1998).
- [17] T.O. Hushcha, A.I. Luik, Yu.N. Naboka, *Talanta* **53**, 29 (2000).
- [18] M.A. Kiselev, Iu. A. Gryzunov, G.E. Dobretsov, Komarova M.N., *Biofizika*, **46**(3), 423 (2001).
- [19] <http://www.nlm.nih.gov/medlineplus/ency/imagepages/1220.htm>, retrieved on July 12, 2010.
- [20] D. Chicea, *Nanoparticles and Nanoparticle Aggregates Sizing by DLS and AFM*, *Optoelectron. Adv. Mater. – Rapid Commun* **4**(9), 1310, (2010).